



Crystal Density Prediction, Charge Density Distribution and the Explosive Properties of the Highly Energetic Molecule 2-Methyl-5-nitramino-tetrazole: a DFT and AIM Study

Ponnusamy SRINIVASAN and Poomani KUMARADHAS*

Department of Physics, Periyar University, Salem 636 011, India

**E-mail: kumaradhas@yahoo.com*

Abstract: The *ab initio* crystal density, bond topological and explosive properties of the energetic molecule 2-methyl-5-nitraminotetrazole (MNAT) have been calculated by the MOLPAK/PMIN software and the AIM theory. The density predicted from the crystal structure simulation almost matches the experimental density. The geometrical parameters of the molecule lifted from the crystal structure are in very close agreement with the reported X-ray molecular structure. The bond topological analysis predicts a significantly low bond electron density, as well as a less Laplacian of electron density, for the N–NO₂ bond. The Laplacian for the bond to the attached methyl group, the C(2)–N(2) bond, is also found to be less negative; the less negative values of the Laplacian confirms that these are the weakest bonds in the molecule. The impact sensitivity (h_{50}) of the molecule has been calculated, and is almost equal to the reported experimental value. The sensitivity of the molecule was also estimated from the electrostatic imbalance parameter and has the value $v = 0.242$. The isosurface of the electrostatic potential of the molecule displays a high negative electrostatic potential region around the tetrazole ring and the nitramine N–N bond, which are the possible reactive locations in the molecule.

Keywords: crystal density, electron density, Laplacian of electron density, impact sensitivity, electrostatic potential

Introduction

The development of new, less sensitive, energetic materials is an emerging area of materials chemistry [1]. The general requirements for these potential

high energy, density materials (HEDMs) includes (i) high density and energy; (ii) thermal stability/storability; (iii) low handling hazards (*e.g.*, low sensitivity to impact, friction, electrostatic discharge, and low toxicity); and (iv) simple cost effective production routes (*i.e.*, three or less synthetic steps) [2, 3] and so on. In the continuous search for novel green energetic materials with high nitrogen and low carbon content, there are currently several groups across the world involved in designing HEDMs based on tetrazoles [4]. Tetrazole based energetic materials are a new class of energetic materials and have received a substantial amount of interest over recent years [5]. These tetrazole type energetic materials have various applications such as low-smoke producing pyrotechnic compositions, gas generators, propellants and high explosives [6]. The tetrazole ring has four nitrogen atoms and one carbon atom and it has been reported that this ring is thermodynamically stable, as demonstrated by the fact that it is recovered unchanged after long periods of heat treatment [7, 8]. The 2-methyl-5-nitramino-tetrazole molecule (MNAT) is one of the most promising classes of tetrazole molecules (Figure 1). Nitraminotetrazoles are five-membered aromatic heterocycles with a nitramine substituent, and are one of the important classes of new energetic materials [9]. Most tetrazole compounds exhibit positive heats of formation owing to their high nitrogen content and to their excellent thermal stabilities arising from their aromaticity [10]. MNAT was first prepared and characterized nearly 50 years ago [11], but recently Klapötke *et al.* reported the synthesis, X-ray structure and detonation properties of MNAT [12].

Detonation is a very important explosive property; generally, the explosive power of an energetic material largely depends on the density of the material [13]. To obtain such high density materials through trial synthesis is not a straight forward procedure, and moreover it is hazardous. Alternatively, prior to synthesis, the density can be predicted from the *ab initio* crystal structure via computational techniques and this may be a viable route to obtain the exact density of the material [14].

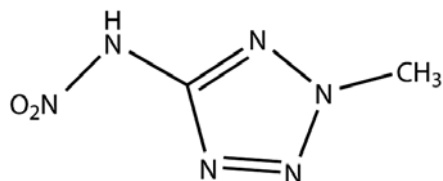


Figure 1. Chemical structure of 2-methyl-5-nitraminotetrazole.

Since, the energetic nature of explosives is mainly influenced by the packing mode of the molecules (density), increasing the density of the material would

be a primary objective for designing highly energetic materials. The strength of the bonds in the molecule needs to be checked, as it is directly related to the initiation of detonation and it determines, in part, the sensitivity of the molecule. In this context, bond topological characterization allows the bond strength (strong and weak bonds) of molecules at the electronic level to be understood. Our recent studies on various energetic molecules explore the identification of the weakest bonds in the molecule by bond topological characterization [15, 16]. The sensitivity of an energetic material to external stimuli is also one of the key properties of energetic materials and it has potential importance for the handling of explosive materials [17]. Hence, to understand the sensitivity (shock, impact and heat) of energetic materials, the above properties are essential. The main aims of the present study are to (i) predict the density of energetic materials from the *ab initio* crystal structure, (ii) determine the bond topological and electrostatic properties from quantum chemical calculations and AIM (Atoms in Molecules) theory [18], and (iii) estimate other possible energetic properties by computational techniques. These energetic parameters certainly enable the density and the sensitivity of the materials to be predicted. This new strategy of computational study may be useful for designing new novel energetic materials prior to experimental attempts (synthesis and tests) which may be hazardous. Furthermore the risk inherent in synthesising many molecules is reduced to perhaps just one selected potential molecule.

Materials and Methods

Ab initio crystal structure and density

Crystal density is an essential parameter, which decides the detonation power of an explosive material. According to Kamlet and Jacobs' [19] semi-empirical equations, the detonation velocity (V) of most energetic materials increases with increasing density. Hence, for better performance, the density of materials is an important parameter. We have predicted the density of the title molecule from its *ab initio* crystal structure using MOLPAK/PMIN software [20-22]. The optimized molecular structure of the MNAT molecule from B3LYP/6-31G* calculations was taken as an initial geometry for the crystal density calculation. MOLPAK generated all possible packing arrangements for the reasonable space groups (P-1, $P2_1/c$, $P2_1$, $P2_12_12_1$ and Pbc a) with global minima in the lattice energy surface using the UMD potential [23]. MOLPAK predicted a monoclinic unit cell with the space group $P2_1/c$. Thus the predicted crystal structure is almost identical to the experimental structure [12], with a maximum error of $\sim 0.17\%$.

The unit cell parameters of the predicted crystal structure are: $a = 9.438$, $b = 7.868$, $c = 8.441$ Å with inter-axial angles: $\alpha = \gamma = 90^\circ$, $\beta = 110.3^\circ$. These unit cell parameters are well matched with the reported X-ray structure (Table 1). The calculated lowest energy and highest density of the predicted MNAT molecule are also presented in Table 1. Both the X-ray and the predicted molecule are found in the monoclinic ($P2_1/c$) space group. The density of the predicted structure (1.664 g/cm³) is comparable to the experimental crystal density (1.667 g/cm³).

Table 1. X-ray and predicted crystal structure data (B3LYP/6-31G* level) of the MNAT molecule

	X-ray	Predicted
Formula	C ₂ H ₄ N ₆ O ₂	C ₂ H ₄ N ₆ O ₂
Crystal System	Monoclinic	Monoclinic
Space group	P2 ₁ /c	P2 ₁ /c
Density (g/cm ³)	1.667	1.664
Cell volume (Å ³)	574.12	587.6
Lattice Parameters		
a (Å)	9.527	9.438
b (Å)	7.73	7.868
c (Å)	8.459	8.441
$\alpha/\beta/\gamma$ (°)	90/112.8/90	90/110.3/90

In order to determine the bond topological and electrostatic properties of the MNAT molecule a single point energy calculation was carried out for molecules lifted from the X-ray and the predicted crystal structure. These calculations were carried out using the B3LYP method [24] with the basis set 6-31G* using the Gaussian03 program [25]. The wave function obtained from the single point energy calculation was used to calculate the bond topological properties, such as bond electron density, Laplacian of electron density, and bond ellipticity at the bond critical points using the Bader's theory of Atoms in Molecules (AIM) implemented in the AIMALL software [26]. The deformation density of the molecule was plotted using the software *wfn2plots* and *XD* packages [27]. The deformation density of the molecule is defined as $\Delta\rho(\mathbf{r}) = \rho_{\text{mol}}(\mathbf{r}) - \rho_{\text{ref}}(\mathbf{r})$, where $\rho_{\text{mol}}(\mathbf{r})$ is the electron density of the molecule and $\rho_{\text{ref}}(\mathbf{r})$ is the reference density of the molecule. The reference density distribution is the density of the neutral spherical ground state atom at each nuclear position of the bond [28]. The molecular electrostatic potential map was plotted with *MOLISO* [29] software in order to visualize the electropositive and electronegative regions of the molecule.

Results and Discussion

Structural aspects

Figure 2 shows the geometry of the molecule lifted from the predicted crystal structure. Its geometrical parameters are compared with the reported X-ray structure (Table 2). The N–N bond distances in the tetrazole ring of the predicted molecule range from 1.309 to 1.335 Å; these distances are almost equal to those in the reported structure (1.319–1.328 Å) [12]. The N–N bond distance in the nitramine group (1.423 Å) is longer than the N–N bonds (~1.324 Å) in the tetrazole ring. The C–N bond distances of the tetrazole ring are ~1.343 Å, which is very close to those of similar reported experimental structures (1.332 Å) [12]. The bond distance of the C(2)–N(2) bond is 1.454 Å, which is slightly longer than the ring C–N bonds; this variation may be due to the effect of the methyl group attached to the C(2)–N(2) bond. The C–H bond distances (Table 2) are slightly longer than the experimental ones [12], with a maximum deviation of ~0.16 Å. The bond angles are also very similar to those in the reported X-ray structure, with a maximum difference for non-hydrogen bonded atoms of 2°. The bonds attaching the nitramine and methyl groups to the ring are twisted, particularly, that for the N–NO₂ group which does not lie in the plane of the tetrazole ring. This can be readily seen from the torsion angle of the C(1)–N(5)–N(6)–O(2) bonds (~22.19°).

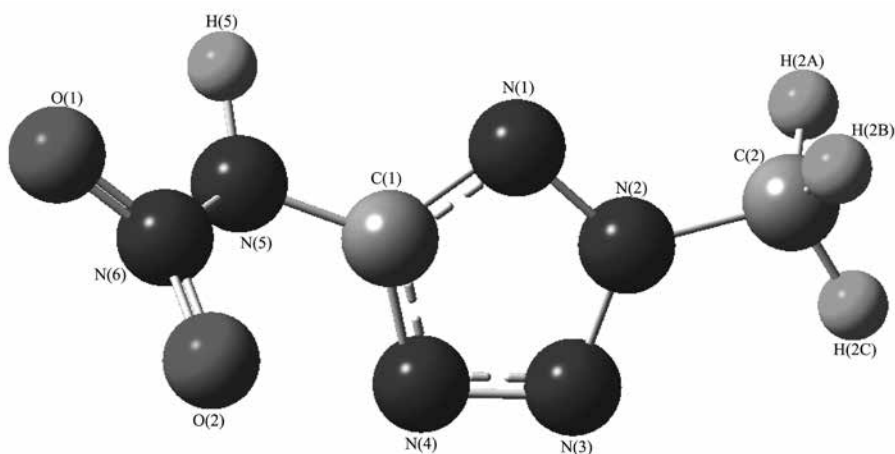


Figure 2. Energy minimized structure of the predicted 2-methyl-5-nitramino-tetrazole molecule.

Table 2. Geometric parameters

Bond lengths (Å)		Bond angles (°)		Torsion angles (°)	
X-ray	Predicted	X-ray	Predicted	X-ray	Predicted
N(1)-N(2)	1.322	N(3)-N(2)-N(1)	106.0	N(1)-N(2)-N(3)-N(4)	1.0
N(2)-N(3)	1.319	N(4)-N(3)-N(2)	123.9	N(3)-N(2)-N(1)-C(1)	-0.4
N(3)-N(4)	1.328	C(1)-N(1)-N(2)	105.8	N(1)-N(2)-N(3)-C(2)	-177.8
C(1)-N(1)	1.339	C(1)-N(4)-N(3)	101.1	N(1)-C(1)-N(4)-N(3)	0.9
C(1)-N(4)	1.325	N(4)-C(1)-N(1)	113.2	N(5)-C(1)-N(1)-N(2)	-176.8
C(1)-N(5)	1.397	N(5)-C(1)-N(1)	122.3	N(2)-N(3)-N(4)-C(1)	-1.1
C(2)-N(2)	1.459	N(5)-C(1)-N(4)	124.5	N(1)-C(1)-N(5)-N(6)	-110.4
N(5)-N(6)	1.379	C(1)-N(5)-N(6)	117.9	N(4)-C(1)-N(5)-N(6)	73.5
N(6)-O(1)	1.224	C(2)-N(2)-N(1)	114.1	N(5)-C(1)-N(4)-N(3)	177.2
N(6)-O(2)	1.217	C(2)-N(2)-N(3)	122.1	N(4)-C(1)-N(1)-N(2)	-0.3
N(5)-H(5)	0.857	N(5)-N(6)-O(1)	115.6	C(2)-N(3)-N(4)-C(1)	177.7
C(2)-H(2A)	0.930	N(5)-N(6)-O(2)	118.2	O(2)-N(6)-N(5)-H(5)	-159.2
C(2)-H(2B)	0.921	O(1)-N(6)-O(2)	126.2	O(2)-N(6)-N(5)-C(1)	-19.2
C(2)-H(2C)	0.960	C(1)-N(5)-H(5)	118.4	O(1)-N(6)-N(5)-H(5)	23.8
		N(6)-N(5)-H(5)	110.2	O(1)-N(6)-N(5)-C(1)	163.8
		N(2)-C(2)-H(2A)	107.9	H(2C)-C(2)-N(3)-N(2)	-140.1
		N(2)-C(2)-H(2B)	109.2	H(2C)-C(2)-N(3)-N(4)	41.2
		N(2)-C(2)-H(2C)	108.7	H(2B)-C(2)-N(3)-N(4)	-77.8
		H(2A)-C(2)-H(2B)	109.5	H(2B)-C(2)-N(3)-N(2)	100.9
		H(2A)-C(2)-H(2C)	112.3	H(2A)-C(2)-N(3)-N(2)	-18.1
		H(2B)-C(2)-H(2C)	109.2	H(2A)-C(2)-N(3)-N(4)	163.3
				N(1)-C(1)-N(5)-H(5)	26.3
				N(4)-C(1)-N(5)-H(5)	-149.8
					-152.9

Charge density distribution

The charge density distribution of the molecule has been determined using AIM theory [30]. Specifically, in order to calculate the electron density at the bond critical point (bcp) of each bond in the molecule, a critical point analysis has been carried out. A (3,-1) type of bcp was found for all bonds in the molecule lifted from the crystal structure of the reported X-ray as well as the predicted crystal structures. The bond topological parameters of electron density at the bcp of each bond were determined (Table 3). The electron density distribution pattern of the predicted structure was in close agreement with the reported X-ray model. Figure 3 shows the deformation density map of the molecule drawn from the predicted crystal structure. The charge accumulation in the N(3)–N(4) bond [$2.79 \text{ e}\text{\AA}^{-3}$] is slightly higher than that in the other two N–N bonds [N(1)–N(2): 2.63 and N(2)–N(3): $2.62 \text{ e}\text{\AA}^{-3}$] of the tetrazole ring and slightly lower when compared with the similar dimethylnitraminotetrazole molecule.

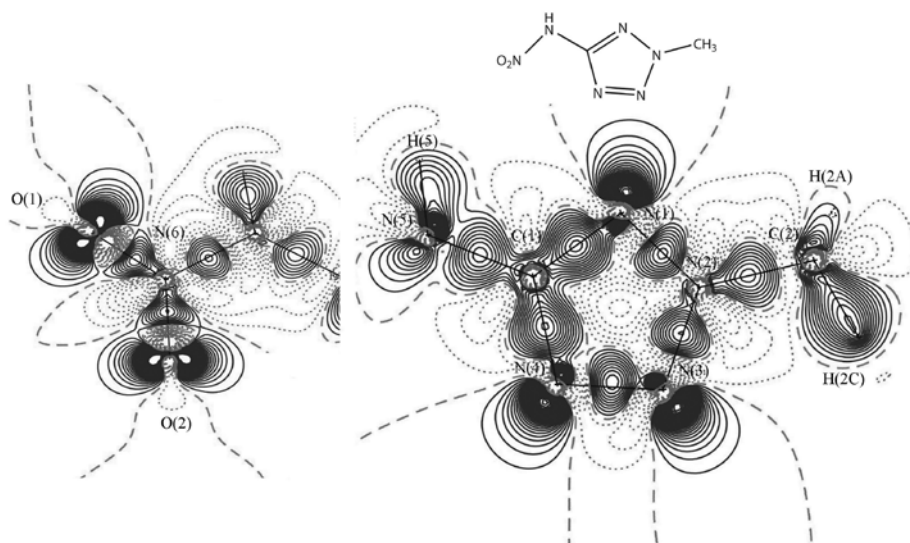


Figure 3. Deformation of electron density of the 2-methyl-5-nitraminotetrazole (MNAT) molecule. The positive contours (solid lines) and negative contours (dotted lines) are drawn at $0.05 \text{ e}\text{\AA}^{-3}$ intervals. The zero contours are dashed lines.

Furthermore, the N–N bond density of the tetrazole ring was found to be significantly higher than the nitro group of the nitramine group [$2.17 \text{ e}\text{\AA}^{-3}$], the low $\rho_{\text{bcp}}(\mathbf{r})$ of the N–NO₂ bond being due to the effect of the NO₂ group; this value

is almost equal to the corresponding value in the RDX molecule ($\sim 2.14 \text{ e}\text{\AA}^{-3}$). The bond density of the C–N bonds of the tetrazole ring was found to be equal, with a value of $\sim 2.36 \text{ e}\text{\AA}^{-3}$; this density is almost identical to that reported for a similar structure [31]. The bond density of the C–N bond attaching a methyl group was $\sim 1.74 \text{ e}\text{\AA}^{-3}$, which is almost equal to the value in the X-ray structure ($1.70 \text{ e}\text{\AA}^{-3}$). The $\rho_{\text{bcp}}(r)$ of the N–O bonds was found to be very high (ranging from 3.38 to $3.42 \text{ e}\text{\AA}^{-3}$), with the electron density concentrated mainly in the non-bonding direction, emphasizing the lone pair regions (Figure 3).

Table 3. Selected bond topological parameters and the energy density distribution of the predicted (first line) and X-ray (second line) structure of the MNAT molecule

Bonds	$\rho_{\text{bcp}}(r)^a$	$\nabla^2\rho_{\text{bcp}}(r)^b$	ε^c	d_1^d	d_2^d	D^d	$V(r)^e$	$G(r)^e$	$H(r)^e$
N(1)–N(2)	2.630	-18.3	0.14	0.636	0.692	1.328	1.52	-4.32	-2.80
	2.710	-20.2	0.12	0.650	0.674	1.325	1.52	-4.46	-2.94
N(2)–N(3)	2.620	-17.8	0.20	0.639	0.697	1.336	1.52	-4.29	-2.77
	2.720	-19.5	0.20	0.632	0.688	1.320	1.59	-4.55	-2.96
N(3)–N(4)	2.790	-21.4	0.13	0.643	0.669	1.312	1.59	-4.68	-3.09
	2.630	-18.2	0.14	0.634	0.694	1.328	1.53	-4.33	-2.80
C(1)–N(1)	2.390	-23.2	0.34	0.463	0.517	1.333	2.38	-6.39	-4.01
	2.410	-28.9	0.29	0.847	0.493	1.341	1.82	-5.66	-3.84
C(1)–N(4)	2.360	-29.0	0.27	0.836	0.870	1.354	1.51	-5.05	-3.54
	2.430	-23.4	0.34	0.459	0.867	1.326	2.48	-6.59	-4.11
N(5)–C(1)	2.050	-24.1	0.12	0.878	0.521	1.399	1.22	-4.12	-2.90
	2.040	-23.9	0.11	0.882	0.516	1.398	1.26	-4.19	-2.93
N(2)–C(2)	1.740	-15.3	0.02	0.944	0.694	1.453	1.36	-3.78	-2.42
	1.690	-12.6	0.04	0.948	0.510	1.458	1.44	-3.76	-2.32
N(5)–N(6)	2.170	-13.0	0.24	0.729	0.510	1.423	1.09	-3.08	-1.99
	2.390	-16.0	0.25	0.709	0.671	1.379	1.22	-3.55	-2.33
N(6)–O(1)	3.380	-22.6	0.11	0.629	0.594	1.223	2.67	-6.91	-4.24
	3.370	-22.4	0.11	0.629	0.595	1.224	2.65	-6.87	-4.22
N(6)–O(2)	3.420	-23.3	0.11	0.627	0.590	1.217	2.72	-7.08	-4.36
	3.430	-23.5	0.11	0.591	0.626	1.217	2.71	-7.07	-4.36

^a The electron density $\rho_{\text{bcp}}(\text{e}\text{\AA}^{-3})$; ^b Laplacian $\nabla^2\rho_{\text{bcp}}(\text{e}\text{\AA}^{-5})$; ^c ε is the bond ellipticity; ^d d_1 and d_2 are the distances in \AA between CP and the respective atoms of the bond; ^e Energy density distribution ($\text{H}\text{\AA}^{-3}$).

Laplacian of electron density and energy density

The type of interaction existing between the atoms in molecules can be well confirmed by a detailed investigation of the Laplacian of electron density $\nabla^2\rho_{\text{bcp}}(\mathbf{r})$, which provides the necessary information about the charge concentration/depletion at the bcp of the chemical bonds in the molecule [32]. Figure 4, displays the Laplacian of electron density $\nabla^2\rho_{\text{bcp}}(\mathbf{r})$ of the MNAT molecule in different planes. The Laplacian of electron density for the N–N bonds in the tetrazole ring varied from -17.8 to $-21.4 \text{ e}\text{\AA}^{-5}$, in which the $\nabla^2\rho_{\text{bcp}}(\mathbf{r})$ of N(2)–N(3) [$-17.8 \text{ e}\text{\AA}^{-5}$] was found to be less negative and indicated that the charges of the bond are more depleted than the other two similar bonds. Unlike the ring N–N bonds, the Laplacian of electron density of the N–N bond of the nitramine was notably less negative, which shows that the bond charges are highly depleted [$\sim -13.0 \text{ e}\text{\AA}^{-5}$]. This was attributed to the effect of the electron rich NO_2 group on the bonding electrons. This high charge depletion indicates that the N– NO_2 bond is the weakest bond in the molecule. Furthermore, we have compared the Laplacian of the N– NO_2 bond with that reported for the dimethylnitraminotetrazole molecule, which is a good match with the MNAT molecule (Table 3). The Laplacian of the C–N bonds [C(1)–N(1): $-23.2 \text{ e}\text{\AA}^{-5}$ and C(1)–N(4): $\sim -29 \text{ e}\text{\AA}^{-5}$] were found to be unequal; the bond charges of the C(1)–N(4) bond were highly concentrated. By contrast, the trend in the non-ring C–N bond is noticeably different, where the bond charges of C(2)–N(2) are not very concentrated and the value is $\sim -15.3 \text{ e}\text{\AA}^{-5}$; this large charge depletion confirmed that the N– CH_3 bond is also a weak bond in the molecule.

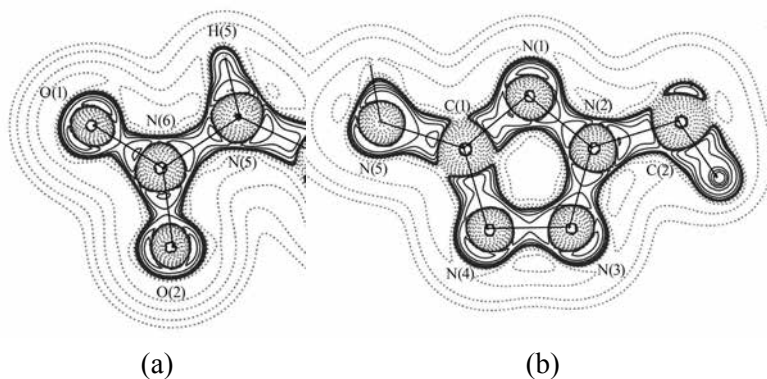


Figure 4. Laplacian of electron density of 2-methyl-5-nitraminotetrazole. (a) Nitramine ($-\text{N}-\text{NO}_2$) fragments and (b) Tetrazole ring. The positive contours are solid lines, negative contours are dotted lines. Contours are drawn on a logarithmic scale, $3.0 \times 2^N \text{ e}\text{\AA}^{-5}$, where $N = 2, 4$, and 8×10^n , $n = -2, -1, 0, 1, 2$.

The potential energy $V(r)$, kinetic energy $G(r)$ and the total energy density $H(r)$ distribution of the molecule were also calculated in order to understand the energy density distribution of the MNAT molecule in the crystal [33]. The total energy density distribution of the N–N bonds [$\sim 2.8 \text{ H}\text{\AA}^{-3}$] in the tetrazole ring are almost equal except for the N(3)–N(4) bond [$\sim 3.09 \text{ H}\text{\AA}^{-3}$] (Table 3). The energy density of the ring C–N bonds [$\sim 4.0 \text{ H}\text{\AA}^{-3}$] is higher compared to the other C–N bond in the molecule. The nitro group N–O bonds [$\sim 4.24 \text{ H}\text{\AA}^{-3}$] carry the highest energy density in the molecule. The energy density distribution of all bonds is presented in Table 3. Furthermore, to confirm the strength (weak or strong) of the bond, we have calculated the bond dissociation energy (BDE) of the molecule, in which the BDE of the nitramine group (N–NO₂) is 33.59 Kcal/mol. According to Chung et al's criteria [34], the BDE for a stable bond must be more than 20 Kcal/mol. In this context, the predicted value of the BDE for the MNAT molecule met the above criteria, and hence this molecule may be considered as a stable energetic molecule.

Impact sensitivity and molecular stability

The impact sensitivity of MNAT has been calculated from the NO₂ group charges and the oxygen balance (OB) of the molecule [35]. The nitro group charge ($-Q_{NO_2}$) has been calculated from the sum of the net atomic charges of the nitrogen (Q_N) and oxygen atoms (Q_{O1} and Q_{O2}) of the nitro group.

$$-Q_{NO_2} = Q_N + Q_{O1} + Q_{O2}$$

The calculated group charge ($-Q_{NO_2}$) was 0.142e, which is significantly less compared with the values reported for TNT [2,3,4-Trinitrotoluene] (0.249e) and FOX-7 (0.365e) [36]. Furthermore, the oxygen balance (OB%) [37] of MNAT was also calculated, and found to be negative (-44.41%). This value for the OB and the NO₂ group charge of the molecule facilitates an understanding of the effect of molecular structure on the impact sensitivity and enables the impact sensitivity (h_{50}) of the molecule to be calculated [35].

$$h_{50} = 0.1926 + 98.64Q_{NO_2}^2 - 0.03405OB_{100}$$

The predicted h_{50} value is 3.6 m, which is somewhat less than the value from the X-ray structure (5.0 m). This value was then compared with those of some reported explosives (Table 4) [36-38].

Table 4. Impact sensitivity (h_{50}) and the energy gap of the MNAT molecule and other energetic molecules

Molecule	OB% ⁽³⁷⁾	Q_{NO_2}	h_{50} (m)	HOMO (eV)	LUMO (eV)	$\Delta E_{HOMO-LUMO}$ (eV)
MNAT Predicted	-44.41	0.139	3.61	7.86	1.79	6.07
MNAT X-ray	-44.41	0.184	5.04 (exp)	8.00	1.65	6.35
RDX ⁽³⁸⁾	-21.61	-0.029	1.01	7.10	3.29	3.81
TNT ⁽¹⁶⁾	-73.96	0.249	8.82	7.89	2.99	4.90
TNB ⁽³⁷⁾	-56.31	-0.360	14.8	9.90	4.89	5.01
TATB ⁽¹⁵⁾	-55.78	-0.510	27.7	7.10	3.29	3.81

The band gap between the highest occupied molecular orbital (HOMO) and the lowest unoccupied molecular orbital (LUMO) gives information about the stability of explosives [39]. Furthermore, the principle of easiest transition (PET) states that the smaller the band gap ($\Delta E_{LUMO-HOMO}$) between HOMO and LUMO, the easier is the electron transition and the lower the stability [40]. Therefore in the present study, we have estimated the band gap for the predicted and the X-ray structures of MNAT; the values were 6.35eV and 6.07eV respectively. These predicted values are larger than those reported for the energetic molecules TNB (5.01 eV), TNT (4.92 eV), TATB (3.8 eV) and RDX (3.81 eV), and indicates that MNAT is more stable than these other molecules (Table 4).

Electrostatic potential

The molecular electrostatic potential (MEP) explores the polarization, electron correlation, charge transfer effect and the reaction sites of the molecule [41]. Figure 5, shows the electrostatic potential of the molecule plotted for the isosurface values $\pm 0.5 \text{ e}\cdot\text{\AA}^{-1}$. A large electronegative region is found near the nitrogen rich region [N(2), N(3) and N(4) atoms] of the tetrazole ring, which is found to be much higher than the electronegative region found in the vicinity of the NO_2 group. These two regions are the expected nucleophilic sites of the molecule.

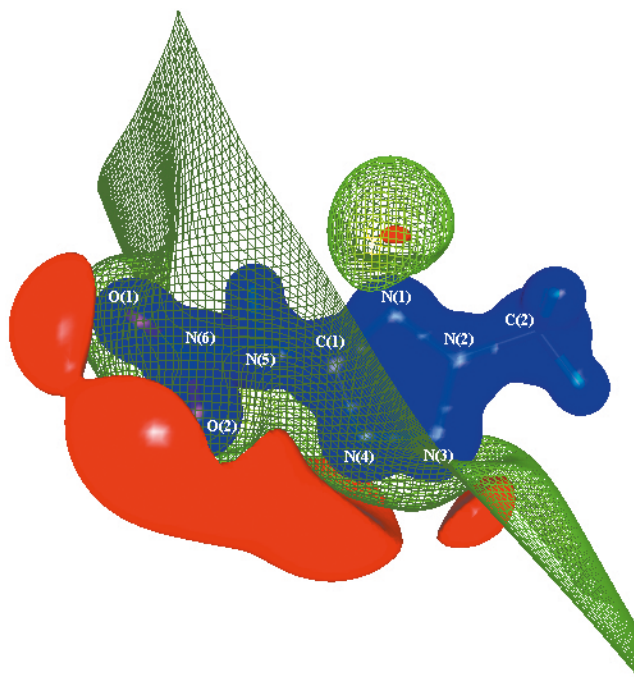


Figure 5. Isosurface representation of the electrostatic potential of the MNAT molecule. Blue indicates the electropositive regions and red indicates electronegative regions. Isosurface values are $\pm 0.5 \text{ e}\text{\AA}^{-1}$.

Furthermore, the sensitivities of energetic molecules are also related to the anomalous charge imbalance, which characterizes the balance between positive and negative surface potentials as the parameter (v) [42].

$$v = \frac{\sigma_+^2 \cdot \sigma_-^2}{(\sigma_+^2 + \sigma_-^2)^2}$$

The quantities σ_+^2 and σ_-^2 are the indicators of the strength and variability of the positive and negative surface potentials. Here, we have calculated the positive and negative electrostatic potential variances (σ_+^2 and σ_-^2) and the electrostatic balance parameter (v) of the predicted MNAT molecule; the corresponding values are $\sigma_+^2 = 112.54$, $\sigma_-^2 = 78.38 \text{ (Kcal/mol}^{-1}\text{)}^2$, with $v = 0.242$, respectively. This v value is close to the balance parameter of a stable molecule ($v = 0.25$) [43], and indicates that MNAT is presumably an electrostatically stable molecule.

Conclusions

In the present study, we have predicted the density, bond strength, bond topological and the electrostatic properties, and the impact sensitivity of the MNAT molecule from quantum chemical calculations coupled with AIM theory. The electrostatic parameters characterize well the energy density and sensitivity of the MNAT molecule. The predicted crystal density is found to be very close to the experimentally reported crystal density. This confirms that the density of energetic materials can be predicted prior to synthesis. However, the density prediction for a new molecule requires proper experimental validation. The bond topological analysis precisely characterizes the electron density of the trigger nitro group of the N–NO₂ group as it is highly depleted and the nitramine N–N is considered as the weakest bond in the molecule; by contrast, the N–N bonds in the tetrazole ring are found to be very strong. The C–N bond attaching the methyl group is also weak. Furthermore, the bond sensitivity calculated from the nitro group charges and the oxygen balance, shows that the N–N bond of the nitramine is more sensitive than all the other bonds in the molecule. Large electronegative regions are found in the molecule near to the nitrogen rich area of the ring as well as in the vicinity of the NO₂ group; these are the expected nucleophilic sites of the molecule. The fine details which we have provided for the energetic MNAT molecule at the electronic level, may facilitate the design of other tetrazole-based, high energy, high density materials in the future.

References

- [1] Sikder A.K., Sikder N., A Review of Advanced High Performance, Insensitive and Thermally Stable Energetic Materials Emerging for Military and Space Applications, *J. Hazard. Mater.*, **2004**, *A112*, 1-15.
- [2] Nesprias K.R., Canizo A.I., Eyler N., Mateo C.M., Jorge N.L., Preparation and Thermal Decomposition Reaction of p-Chloro Benzaldehyde Diperoxide in Tetrahydrofuran Solution, *J. Energ. Mater.*, **2007**, *25*, 69-78.
- [3] Bulusu S.N., Chemistry and Physics of Energetic Materials, Kluwer Academic Publishers, Boston, MA, **1989**.
- [4] Cubero E., Orozco M., Luque F.J., Theoretical Study of Azidotetrazole Isomerism: Effect of Solvent and Substituents and Mechanism of Isomerization, *J. Am. Chem. Soc.*, **1998**, *120*, 4723-4731.
- [5] Klapötke T.M., Mayer P., Schulz A., Weigand J.J., 1,5-Diamino-4-methyltetrazolium Dinitramide, *J. Am. Chem. Soc.*, **2005**, *127*, 2032-2033.
- [6] Denffer M.V., Heeb G., Klapötke T.M., Kramer G., Spiess G., Welch J.M., Improved

- Synthesis and X-Ray Structure of 5-Aminotetrazolium Nitrate, *Propellants Explos. Pyrotech.*, **2005**, *30*, 191-195.
- [7] Klapötke T.M., Karaghiosoff K., Mayer P., Penger A., Welch J.M., Synthesis and Characterization of 1,4-Dimethyl-5-aminotetrazolium 5-Nitrotetrazolate, *Propellants Explos. Pyrotech.*, **2006**, *31*, 188-195.
- [8] Hammerl A., Klapötke T.M., Tetrazolypentazoles: Nitrogen-Rich Compounds, *Inorg. Chem.*, **2002**, *41*, 906-912.
- [9] Ebespacher M., Klapötke T.M., Sabate C.M., Nitrogen-Rich Alkali Metal 5,5'-Hydrazinebistetrazolate Salts: Environmentally Friendly Compounds in Pyrotechnic Mixtures, *New J. Chem.*, **2009**, *33*, 517.
- [10] Klapötke T.M., Stierstorfer J., Wallek A.U., Nitrogen-Rich Salts of 1-Methyl-5-nitriminotetrazolate: An Auspicious Class of Thermally Stable Energetic Materials, *Chem. Mater.*, **2008**, *20*, 4519-4530.
- [11] Klapötke T.M., Mayer P., Verma V., Synthesis and Characterization of 1-Azido-2-nitro-2-azapropane and 1-Nitrotetrazolato-2-nitro-2-azapropane, *Propellants Explos. Pyrotech.*, **2006**, *31*, 263-268.
- [12] Klapötke T.M., Stierstorfer J., Nitration Products of 5-Amino-1*H*-tetrazole and Methyl-5-amino-1*H*-tetrazoles – Structures and Properties of Promising Energetic Materials, *Helvetica Chim. Acta*, **2007**, *90*, 2132-2150.
- [13] Badgajar D.M., Talawar M.B., Asthana S.N., Mahulikar P.P., Advances in Science and Technology of Modern Energetic Materials: An Overview, *J. Hazard. Mater.*, **2008**, *151*, 289-305.
- [14] Ammon H.L., Du Z., Holden J.R., *9th Annual Working Group Institute on Synthesis of High Energy Density Proceedings*, Kiamesha Lake, NY, **1990**, 47-61
- [15] David Stephen A., Srinivasan P., Kumaradhas P., Bond Charge Depletion, Bond Strength and the Impact Sensitivity of High Energetic 1,3,5-Triamino-2,4,6-trinitrobenzene (TATB) Molecule: A Theoretical Charge Density Analysis, *Comput. Theo Chem*, **2011**, *967*, 250-256.
- [16] David Stephen A., Pawar R.B., Kumaradhas P., Exploring the Bond Topological Properties and the Charge Depletion-Impact Sensitivity Relationship of High Energetic TNT Molecule via Theoretical Charge Density Analysis, *J. Mol. Struct. (THEOCHEM)*, **2010**, *959*, 55-61.
- [17] Su X., Cheng X., Meng C., Yuan X., Quantum Chemical Study on Nitroimidazole, Polynitroimidazole and Their Methyl Derivatives, *J. Hazard. Mater.*, **2009**, *161*, 551-558.
- [18] Bader R.F.W., Nguyen-Dang T.T., Quantum Theory of Atoms in Molecules – Dalton Revisited, *Adv. Quantum Chem.*, **1981**, *14*, 63-124.
- [19] Kamlet J.M., Jacobs S.J., *Chemistry of Detonations. I. A Simple Method for Calculating Detonation Properties of C-, H-, N-, O-, Explosives*, U.S Naval Ordnance Laboratory, White oak, Silver Spring, Maryland, **1967**.
- [20] a) Holden J.R., Du Z., Amman H.L., Prediction of Possible Crystal Structures for C-, H-, N-, O-, and F-containing Organic Compounds, *J. Comput. Chem.*, **1993**, *14*, 422-437; b) Cromer D.L., Amman H.L., Holden J.R., Report LA-11142-MS,

- Los Alamos National Laboratory, Los Alamos, NM, **1987**.
- [21] Ammon H.L., *MOLPAK Software Suite and User's Manual*, July Version, University of Maryland, College Park, Maryland, **2007**.
- [22] Busing W.R., *PMIN – A Computer Program to Model Molecules and Crystals in Terms of Potential Energy Functions*, Report ORNL-5747, Oak Ridge National Laboratory, Oak Ridge, **1981**.
- [23] Prasad S.M., Du Z., Albu N., Ammon H.L., University of Maryland, College Park, MD, **2004**.
- [24] Perdew J.P., Density-Functional Approximation for the Correlation Energy of the Inhomogeneous Electron Gas, *Phys. Rev. B*, **1986**, *33*, 8822-8824.
- [25] Frisch M.J., Trucks G.W., Schlegel H.B., Scuseria G.E., Robb M.A., Cheeseman J.R., Montgomery A.J., Vreven T., Kudin K.N., Burant J.C., Millam J.M., Iyengar S.S., Tomasi J., Barone V., Mennucci B., Cossi M., Scalmani G., Rega N., Petersson G.A., Nakatsuji H., Hada M., Ehara M., Toyota K., Fukuda R., Hasegawa J., Ishida M., Nakajima T., Honda Y., Kitao O., Nakai H., Klene M., Li X., Knox J., Hratchian H.P., Cross J.B., Adamo C., Jaramillo J., Gomperts R., Stratmann R.E., Yazyev O., Austin A.J., Cammi R., Pomelli C., Ochterski J.W., Ayala P.Y., Morokuma K., Voth G.A., Salvador P., Dannenberg J.J., Zakrzewski V.G., Dapprich S., Daniels A.D., Strain M.C., Farkas O., Malick D.K., Rabuck A.D., Raghavachari K., Foresman J.B., Ortiz J.V., Cui Q., Baboul A.G., Clifford S., Cioslowski J., Stefanov B.B., Liu G., Liashenko A., Piskorz P., Komaromi I., Martin R.L., Fox D.J., Keith T., Al-Laham M.A., Peng C.Y., Nanayakkara A., Challacombe M., Gill P.M.W., Johnson B., Chen W., Wong M.W., Gonzalez C., Pople J.A., *Gaussian 03, revision B.04*. Gaussian Inc., Pittsburgh, PA, **2005**.
- [26] AIMAll (Version 10.03.25) Todd A. Keith (aim.tkgristmill.com), **2010**.
- [27] Volkov A., Macchi P., Farrugia L.J., Gatti C., Mallinson P., Richter T., Koritsanszky T., XD2006 – a Computer Program for Multipole Refinement, *Topological Analysis of Charge Densities and Evaluation of Intermolecular Energies from Experimental or Theoretical Structure Factors*, Version 5.33. State University of New York at Buffalo, NY; Università di Milano, Italy; University of Glasgow, UK; CNR-ISTM Milano, Italy; Free University of Berlin, Germany, **2007**.
- [28] Gillespie R.J., Popelier P.L.A., *Chemical Bonding and Molecular Geometry*, Oxford University Press, New York, **2001**.
- [29] Hubschle C.B., Luger P., *Molliso – a Program for Colour-Mapped Iso-Surfaces*, *J. Appl. Cryst.*, **2006**, *39*, 901-904.
- [30] Bader R.F.W., Atoms in Molecules, *Acc. Chem. Res.*, **1985**, *18*, 9-15.
- [31] David Stephen A., Srinivasan P., Asthana S.N., Pawar R.B., Kumaradhas P., Crystal Structure Prediction and Charge Density Distribution of High Energetic Dimethylnitraminotetrazole: a First Step for the Design of High Energy Density Material, *Cent. Eur. J. Energ. Mater.*, **2012**, *9*(3), 201-217.
- [32] Cromer D.T., Storm C.B., Structure of 4,4',5,5'-Tetranitro-2,2'-biimidazole Dehydrate, *Acta Crystallogr.*, **1990**, *C46*, 1957-1958.
- [33] Cramer P., Kraka E., A Description of the Chemical Bond in Terms of Local

- Properties of Electron Density and Energy, *Croatica Chemica Acta*, **1984**, *57*, 1259-1281.
- [34] Chung G.S., Schimit M.W., Gordon M.S., An *Ab Initio* Study of Potential Energy Surfaces for N₈ Isomers, *J. Phys. Chem. A*, **2000**, *104*, 5647-5650.
- [35] Zhang C., Shu Y., Huang Y., Zhao X., Dong H., Investigation of Correlation between Impact Sensitivities and Nitro Group Charges in Nitro Compounds, *J. Phys. Chem. B*, **2005**, *109*, 8978-8982.
- [36] Cao C., Gao S., Two Dominant Factors Influencing the Impact Sensitivities of Nitrobenzenes and Saturated Nitro Compounds, *J. Phys. Chem. B*, **2007**, *111*, 12399-12402.
- [37] Hui Liu., Hongchen Du., Guixiang Wang., Xuedong Gong., Theoretical Studies on the Structures, Densities, Detonation Properties and Pyrolysis Mechanism of Energetic Compounds Containing Pyridine Ring, *Struct. Chem.*, **2012**, *23*, 479-486.
- [38] Svensson L., Nyqvist J-O., Westling L., *Crystallization Method for HMX and RDX*, US 4638065, **1987**.
- [37] Ghule V.D., Sarangapani R., Jadhav P.M., Pandey R.K., Computational Design and Structure – Property Relationship Studies on Heptazines, *J. Mol. Model.*, **2011**, *17*, 2927-2937.
- [38] Gobel M., Karaghiosoff K., Klapotke T.M., Piercey D.G., Stierstorfer J., Nitrotetrazolate-2*N*-oxides and the Strategy of *N*-Oxide Introduction, *J. Am. Chem. Soc.*, **2010**, *132*(48), 17216- 17226.
- [39] Owens F.J., Jayasuriya K., Abrahamsen L., Politzer P., Computational Analysis of Some Properties Associated with the Nitro Groups in Polynitroaromatic Molecules, *Chem. Phys. Lett.*, **1985**, *116*, 434-438.
- [40] Felipe A.B., Toro-Labbe A., WgFA: A Suite of Programs to Analyse Wavefunctions, Unpublished Manuscript, **2010**.
- [41] Politzer P., Laurence P.R., Abrahamsen L., Zilles B.A., Sjoberg P., The Aromatic C–NO₂-bond as a Site for Nucleophilic Attack, *Chem. Phys. Lett.*, **1984**, *111*(1), 75-78.